Article

Identification of Time-Varying Parameters of Distributed Hydrological Model in Wei River Basin on Loess Plateau in the Changing Environment

Haizhe Wu [1,2], Dengfeng Liu [2,*], Ming Hao [1,*], Ruisha Li [1], Qian Yang [3], Guanghui Ming [4] and Hui Liu [5]

1   The Second Monitoring and Application Center, China Earthquake Administration, Xi'an 710054, China
2   State Key Laboratory of Eco-Hydraulics in Northwest Arid Region, School of Water Resources and Hydropower, Xi'an University of Technology, Xi'an 710048, China
3   Shaanxi Water Resources and Reservoir Dispatching Center, Xi'an 710004, China
4   Key Laboratory of Water Management and Water Security for Yellow River Basin (Ministry of Water Resources), Yellow River Engineering Consulting Co., Ltd., Zhengzhou 450003, China
5   China Institute of Water Resources and Hydropower Research, Beijing 100038, China
*   Correspondence: liudf@xaut.edu.cn (D.L.); ha_mg@163.com (M.H.)

Abstract: In the watershed hydrological model, the parameters represent the characteristics of the watershed. Usually, the parameters are assumed to be constant in the stable environment. However, in the changing environment, the parameters may change and the constant parameters would not represent the change of the characteristics of the runoff generation and routing in the watershed. The identification of the time-varying characteristics of the watershed hydrological model parameters will help to improve the performance of the simulation and prediction of hydrological models in changing environments. Based on the measured data at the ground stations in the Wei River Basin on the Loess Plateau in China, the temporal and spatial evolution of the ecohydrological and meteorological factors was analyzed, and the SWAT model was used to identify the relationship between the model parameters and the factors, such as precipitation, potential evapotranspiration, NDVI and the other environmental characterization factors of the river basin. The results showed that the annual precipitation in the basin showed a decreasing trend, and the annual potential evapotranspiration, the annual average temperature, the annual runoff and the annual average NDVI all showed an increasing trend. The model parameters fluctuated with time during the study period. The change of the soil evaporation compensation coefficient (ESCO) was similar with the annual potential evapotranspiration, and the model parameters all showed a certain correlation with the potential evaporation of the basin, which indicates that the changes of the hydrological model parameters in the upper reach of the Wei River are closely related to the changes of the basin potential evapotranspiration. Potential evapotranspiration is a characterization factor for dynamic changes of the hydrological model parameters in the upper reach of the Wei River.

Keywords: hydrological simulation; time-varying parameters; potential evapotranspiration; Loess Plateau

1. Introduction

In the context of global climate change, the applicability of traditional runoff simulation and forecasting methods has gradually deteriorated, which brings challenges to hydrometeorological simulation and forecasting. The hydrological simulation of the river basin under the changing environment is mainly affected by the climatic conditions and the underlying surface conditions [1]. Climatic conditions are the driving factors of the water cycle in the basin and the prerequisite for the generation of runoff [2], which directly or indirectly affect the runoff process in the basin through changes in factors such as precipitation, evapotranspiration and temperature [3]. Global warming has become an indisputable fact [4]. The rise in temperature will cause changes in other meteorological elements. Significant changes have taken place in the type, intensity and amount of precipitation in many

regions of the world, generally showing that humid regions are becoming more humid, arid regions tend to become more arid and the interannual variability is significantly enhanced [5]. In addition, climatic conditions indirectly affect the hydrological process of the watershed by affecting the growth state of vegetation and its structure [6]. The increase and decrease in watershed runoff is inseparable from the change of the underlying surface conditions. With the promotion of large-scale afforestation and urbanization, surface vegetation coverage conditions and local water and heat flux transfer have undergone dramatic changes [7–10], as well as large-scale water intake [11], water diversion projects and reservoir construction, dispatch operation [12], and so on all leading to sudden changes in natural river runoff. It indicates that the "steady-state" basin assumption in traditional hydrological simulation is facing challenges, so the theory and method of hydrological probability distribution based on the consistency assumption obviously cannot help people accurately reveal the long-term law of water resources and flood evolution in changing environments [13,14]. In the hydrological model, it is generally assumed that the parameters representing the hydrological physical characteristics of the watershed are constant over time, which not only cannot reflect the watershed characteristics correctly, but also seriously weakens the simulation ability of the model. The identification and study of the time-varying characteristics of hydrological model parameters in "unsteady" watersheds, and the establishment of a model parameter estimation method that can reflect the climatic conditions of the watershed and the changing laws of the underlying surface, will improve the simulation and performance of hydrological models in changing environments.

The parameters of the hydrological model are usually closely related to the underlying surface conditions of the watershed, and reflect the hydrological characteristics of the watershed [15]. Since there are significant differences in climatic conditions, geographic locations, vegetation coverage, soil conditions, topography and geological conditions in different watersheds [16,17], the parameter values of the same model will also be very different in different watersheds [18]. In the beginning, the traditional watershed hydrological simulation only considers the spatial variability of the parameters of the hydrological model, but does not consider the dynamic changes of the parameters. Usually, the model parameters are considered to be static and remain unchanged over time in a given period of time. However, under the changing environment, the changes in the characteristics of watershed hydrology are not adequately reflected in the model and such assumptions may no longer be applicable. Many scholars began to question such static assumptions and carried out related researches. Kingumbi et al. [19] simulated the hydrological effect of land-use changes by the MODCOU model in the Merguellil basin in central Tunisia and evaluated the improvement in model representativeness by assigning specific parameters to the production functions in the zones of works of water and soil conservation. Vaze et al. [20] used four different conceptual hydrological models in 61 watersheds in southeastern Australia, and applied the method of segmental calibration to determine the parameter values of the model in each time period, and it was found that climate change during the study period would cause significant dynamic changes of parameters. In 273 watersheds in Austria, Merz et al. [21] identified the dynamic changes of parameters based on the HBV model and found that the changes of model parameters had a strong correlation with environmental meteorological factors such as rainfall, runoff coefficient and potential evapotranspiration. Sun [22] used the THREW model in the upper reach of the Han River, identified that all model parameters had a good correlation with the vegetation index, and proposed a dynamic parameter estimation method based on vegetation coverage, which improved the simulation effect of the model. Under the conditions of increasingly significant changes in the basin environment, the constant model parameters over time will be an important source of simulation errors [23]. Considering the dynamic changes of parameters can significantly improve the simulation effect of the hydrological model for the middle and low water sections of the runoff process [24].

The former studies qualitatively pointed out that the change of river basin environmental factors will cause dynamic changes in model parameters, but did not establish the

quantitative relationship between the factors and the parameters. They mostly focused on the influence of climate variability on the parameters, and ignored the changes in the underlying surface condition. In theory, the underlying surface conditions should have a stronger correlation with the model parameters. Therefore, it is necessary to comprehensively analyze the influence of meteorological factors in the watershed and the changes of the underlying surface conditions on the model parameters, establish a time-varying parameter estimation method based on the watershed characteristics, and further enhance the ability of the hydrological model to reflect the changes of watershed characteristics, in order to significantly improve the watershed characteristics. The study will improve the simulation and prediction effects of hydrological models in changing environments. This study takes the upper reach of the Wei River as the study area, analyzes the temporal and spatial evolution of the ecological hydrometeorological elements in the study area, reveals the temporal and spatial variation of these historical sequences and provides a basis for hydrological simulation. The SWAT model is set up in the study area and the time-varying parameter sequence of the hydrological model is obtained by segmental calibration, and the relationship between the model parameters and environmental characterization factors such as precipitation, potential evapotranspiration and the normalized difference vegetation index (NDVI) is analyzed, which provides a preliminary solution for the improvement of the distributed hydrological model. In Section 2, the study area and data are introduced. In Section 3, the methods and hydrological model are described. In Section 4, the simulation results are displayed. Finally, a conclusion is drawn in Section 5.

2. Study Area and Data

2.1. Study Area

The study area is the upper reach of the Beidao Hydrological Station in the Wei River (Figure 1). The study area is located at $103°97'-106°42'$ E and $34°17'-36°19'$ N, with a catchment area of about 25,000 km^2, accounting for about 19% of the total area of the Wei River Basin. The study area is a Loess hilly and gully area with an altitude of 1079–3934 m. The climate is a continental monsoon climate, with a cold and dry winter and a hot and rainy summer. The average annual precipitation from 1965 to 2017 was 491 mm, and the precipitation was unevenly distributed throughout the year, mostly concentrated in July-September. The annual average temperature is 7.8–13.5 °C, the extreme maximum temperature is 42.8 °C, the extreme minimum temperature is −28.1 °C and the annual potential evapotranspiration is 700–1200 mm.

2.2. Data

In this study, the ground-measured meteorological data include the daily data of 6 meteorological stations and 16 rainfall stations in the study area. The data of the meteorological stations include daily rainfall, temperature, sunshine duration, relative humidity, air pressure and average wind speed. The measured daily runoff data from 2001 to 2017 come from the Beidao Hydrological Station. The location of the stations is shown in Figure 1. The measured flow data and meteorological data come from the *Yellow River Basin Hydrological Yearbook* and the China Meteorological Data Network, respectively. The vegetation data from 2001 to 2017 were derived from the NDVI dataset provided by the MODIS/Terra website. The dataset was the MOD13Q1 product with a spatial resolution of 250 m and a temporal resolution of 16 days.

The DEM data used to build the hydrological model came from the ASTER GDEM data provided by Geospatial Data Cloud (http://www.gscloud.cn, accessed on: 1 October 2022), with a spatial resolution of 30 m. The land use data in 2010 came from the Resource and Environment Data Center of the Chinese Academy of Sciences (http://www.resdc.cn, accessed on: 1 October 2022), and the soil attribute data came from the Harmonized World Soil Database (HWSD), with a spatial resolution of 1000 m. The detailed model construction steps refer to Wu et al. [25].
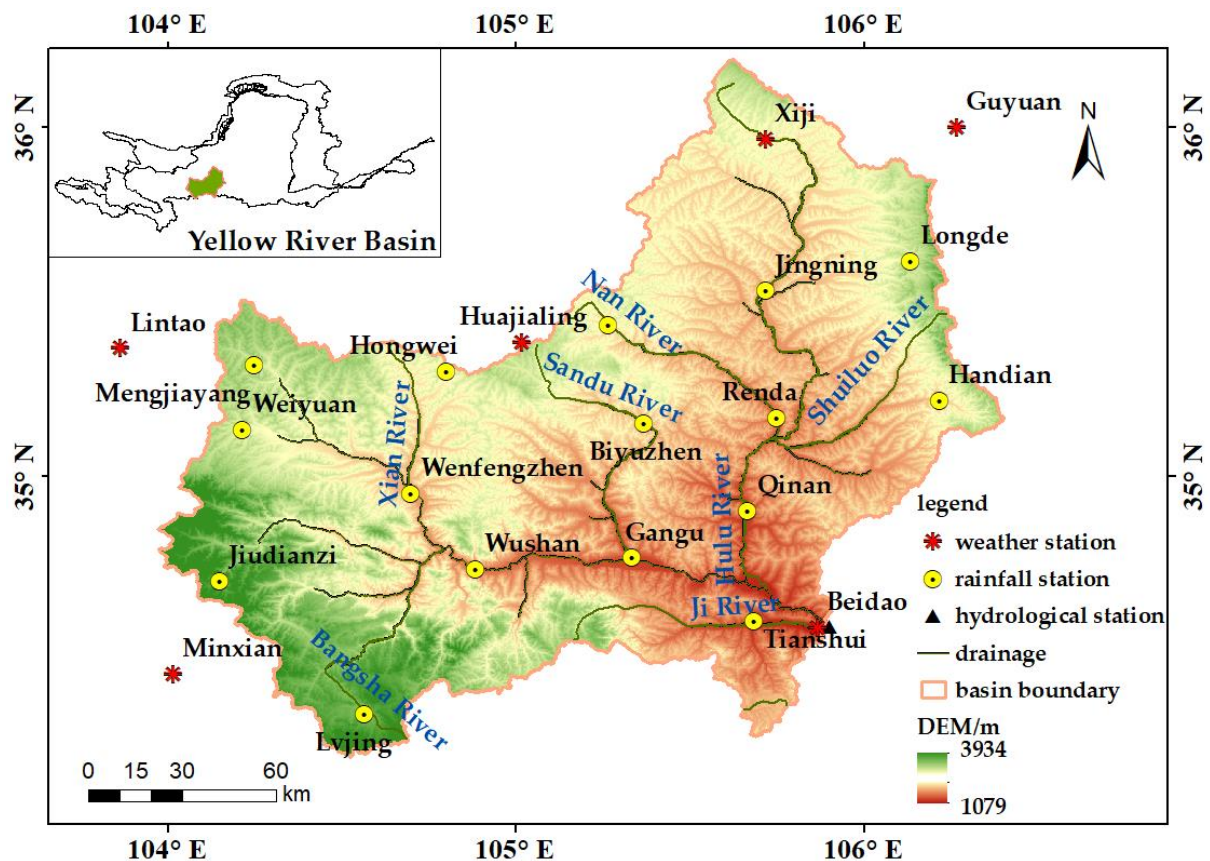
Figure 1. Location of the study area and the stations.

3. Methods

Since there is a lack of recorded solar radiation data at all meteorological stations in the study area, the solar radiation in the watershed was approximated by the number of sunshine hours. The measured meteorological data collected in this study are relatively comprehensive, and the Penman–Monteith method was chosen for the calculation of potential evapotranspiration. For the whole basin average precipitation, potential evapotranspiration, temperature, runoff, vegetation index and other variables in the study area, the linear regression method and the cumulative anomaly method were used to analyze the trend and abrupt change, respectively. The linear regression method is adopted to construct a univariate linear regression equation between the hydrometeorological variable sequence and the time series. The regression coefficient *b* can intuitively reflect the changing rate of the hydrometeorological sequence, and its positive and negative values indicate the increasing or decreasing trend of the hydrometeorological sequence, respectively. The *t*-test method ($a = 0.05$) is used to test the significance of the regression coefficient of the equation; the significance of the change trend of the hydrometeorological sequence is evaluated [26]. The formula of linear regression is as follows:

$$x(t) = a + bt \tag{1}$$

where, *x* is the variable, *t* is time series, *a* and *b* are parameters.

The cumulative anomaly method is a method for evaluating the trend of change according to the increase and decrease in the cumulative anomaly curve. The long-term evolution trend of the hydrometeorological sequence and the approximate time of the sudden change can be evaluated [27]. The formula to calculate the cumulative anomaly value *cd* at time *t* is:

$$cd = \sum_{t=1}^{n} (x(t) - x_{mean}) \tag{2}$$

where, $x(t)$ is the variable at t and x_{mean} is the mean of x.

The SWAT model is a physically based distributed hydrological model and is widely used to simulate the hydrological process of the watershed all over the world. It has great advantages in simulating long-term continuous hydrological processes in large-scale complex watersheds. Therefore, since the model was launched, it has been used in Europe, North America, Canada, Asia and other regions with good results [28,29]. The basin SWAT model was constructed, and the DEM data of the basin were used for catchment analysis and river network extraction. The minimum catchment area threshold was set to 400 km^2, and the study area was divided into 39 sub-basins. Sensitivity analysis was performed using the SUFI-2 algorithm, in which six sensitive parameters were closely related to runoff, such as the number of runoff curves (CN2), the effective hydraulic conductivity of the main channel bed (CH_K2), the soil evaporation compensation coefficient (ESCO), the baseflow α factor of riparian regulation and storage (ALPHA_BNK), the Manning coefficient of the main channel (CH_N2) and the saturated hydraulic conductivity of the soil (SOL_K). Since CH_K2 and SOL_K are parameters that characterize the soil characteristics of the basin, they are not suitable to establish a relationship with the meteorological characteristics, and only CN2, ESCO, ALPHA_BNK and CH_N2 are analyzed.

The Nash–Sutcliffe efficiency coefficient (NSE), the coefficient of determination (R^2) and the Kling–Gupta coefficient (KGE) [30–33] are selected to evaluate the simulated daily flow. The formulas are as follows:

$$\text{NSE} = 1 - \frac{\sum_{i=1}^{n}\left(Q_{o,i} - Q_{s,i}\right)^2}{\sum_{i=1}^{n}\left(Q_{o,i} - \overline{Q}_o\right)^2} \tag{3}$$

$$R^2 = \frac{\sum_{i=1}^{n}\left[\left(Q_{s,i} - \overline{Q}_s\right)\left(Q_{o,i} - \overline{Q}_o\right)\right]^2}{\sum_{i=1}^{n}\left(Q_{o,i} - \overline{Q}_o\right)^2 \sum_{i=1}^{n}\left(Q_{s,i} - \overline{Q}_s\right)^2} \tag{4}$$

$$\text{KGE} = 1 - \sqrt{(r-1)^2 + (\beta-1)^2 + (\gamma-1)^2} \tag{5}$$

$$\beta = \frac{\mu_s}{\mu_o}, \gamma = \frac{\sigma_s/\mu_s}{\sigma_o/\mu_o} \tag{6}$$

where, n represents the length of the runoff sequence; Q_s and Q_o represent the simulated flow and measured flow; μ and σ are the mean and variance, respectively; r is the linear correlation coefficient between the simulated and measured values. The closer NSE and R^2 are to 1, the better the simulation effect is. The KGE coefficient is a comprehensive index including Cv, correlation coefficient and mean value. The closer the value is to 1, the higher the simulation accuracy.

4. Results

4.1. Spatial Distribution of Meteorological Factors

According to the precipitation, air temperature and potential evapotranspiration data calculated by the Penman–Monteith formula from 1965 to 2017 at the six meteorological stations in the upper reach of the Wei River, the spatial distribution of the annual average precipitation, temperature and potential evapotranspiration was plotted by inverse distance weighting interpolation (IDW), as shown in Figure 2. It shows that the annual average precipitation in the basin has obvious differences in spatial distribution, and generally shows a decreasing trend from the southwest of the basin to the northeast. The spatial distribution of the average temperature in the basin shows an increasing trend from the northwest to the southeast. The temperature in about two-thirds of the area is between 6 and 11 °C. From the perspective of the river flow, the high temperature area is located at the outlet of the downstream watershed, and the temperature in the middle and upper reaches of the watershed is lower. It is closely related to the changes of elevation in the basin. The spatial distribution of the annual average potential evapotranspiration in the basin is extremely uneven, and the overall distribution pattern is that the potential evapotranspiration in the

northern part of the basin is slightly larger than that in the southern part of the basin. The spatial distributions of potential evapotranspiration and precipitation are basically opposite; the area with the largest potential evapotranspiration has less precipitation and, on the contrary, the area with the smallest potential evapotranspiration has more precipitation.
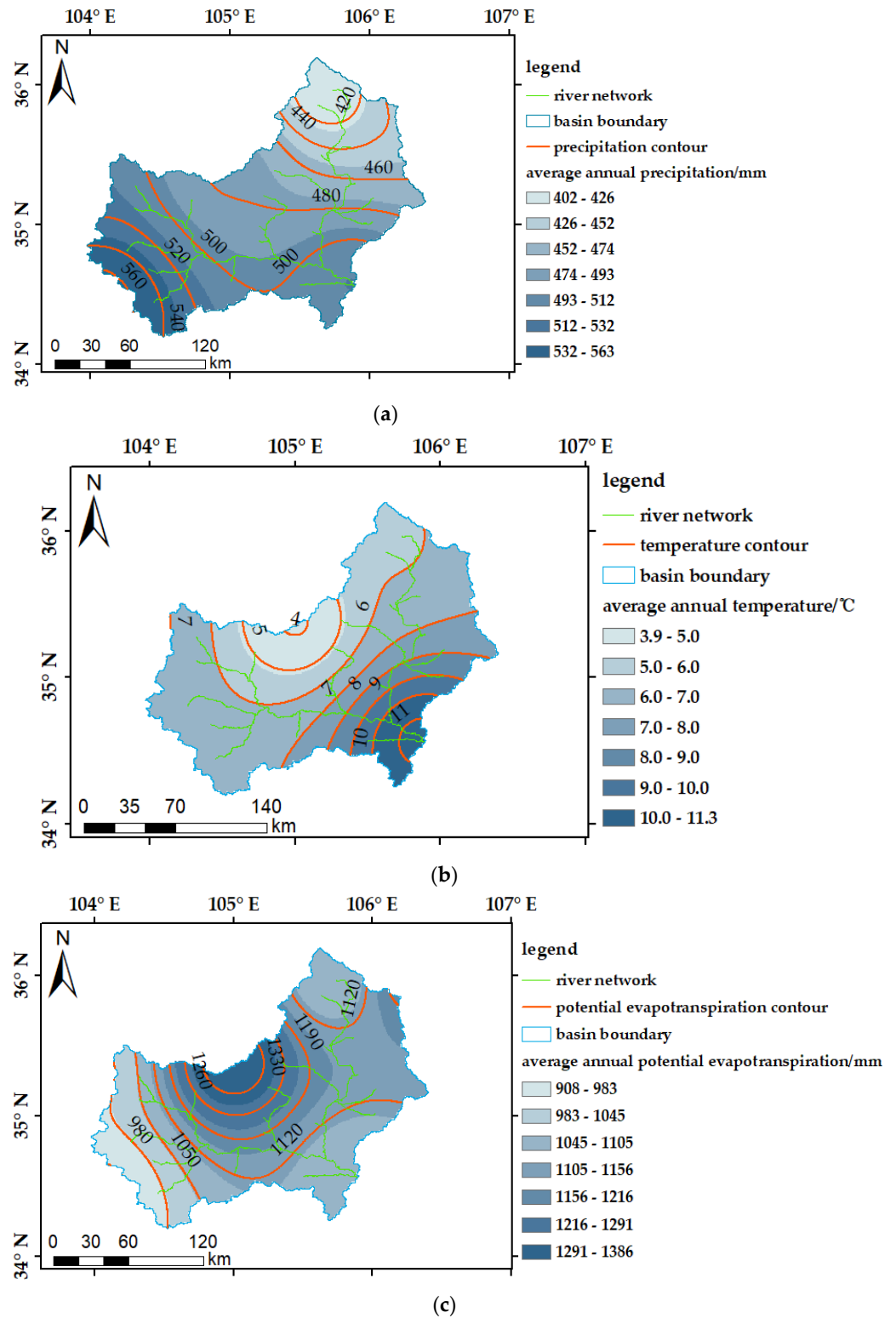
Figure 2. Spatial distribution map of annual average precipitation, temperature and potential evapotranspiration. (**a**) precipitation, (**b**) temperature, (**c**) potential evapotranspiration.

4.2. Interannual Changes of the Environmental Factors

　　The linear regression method was used to analyze the trend of the annual precipitation, temperature, potential evapotranspiration and runoff depth series at the whole basin scale in the study area from 1965 to 2017, and the significance of the trend results was further tested. The results are shown in Figure 3. It shows that the annual precipitation in the basin shows an insignificant decreasing trend, with a decreasing rate of 0.59 mm/a. The mean annual precipitation in the basin was 491.37 mm, the annual precipitation reached the maximum in 1967, about 704.04 mm, and the minimum in 1982. The annual average temperature in the basin shows a significant growth trend, with an increasing rate of 0.03 °C/a. The mean annual temperature in the basin is 6.62 °C. The annual average temperature reached the maximum in 2016, about 7.98 °C, and was the minimum in 1967. The annual potential evapotranspiration in the basin showed a significant increasing trend, with an increasing rate of 1.87 mm/a. The mean annual potential evapotranspiration in the basin was 1150.72 mm, and the annual potential evapotranspiration reached the maximum in 2016, about 1280.31 mm, and was the minimum in 1967. The annual runoff depth of the Beidao Hydrological Station showed an insignificant trend with an increasing rate of 0.42 mm/a. The mean annual runoff depth of the Beidao Hydrological Station was 26.20 mm, and the annual runoff depth reached the maximum in 2013, about 49.01 mm, and was the minimum in 2002.
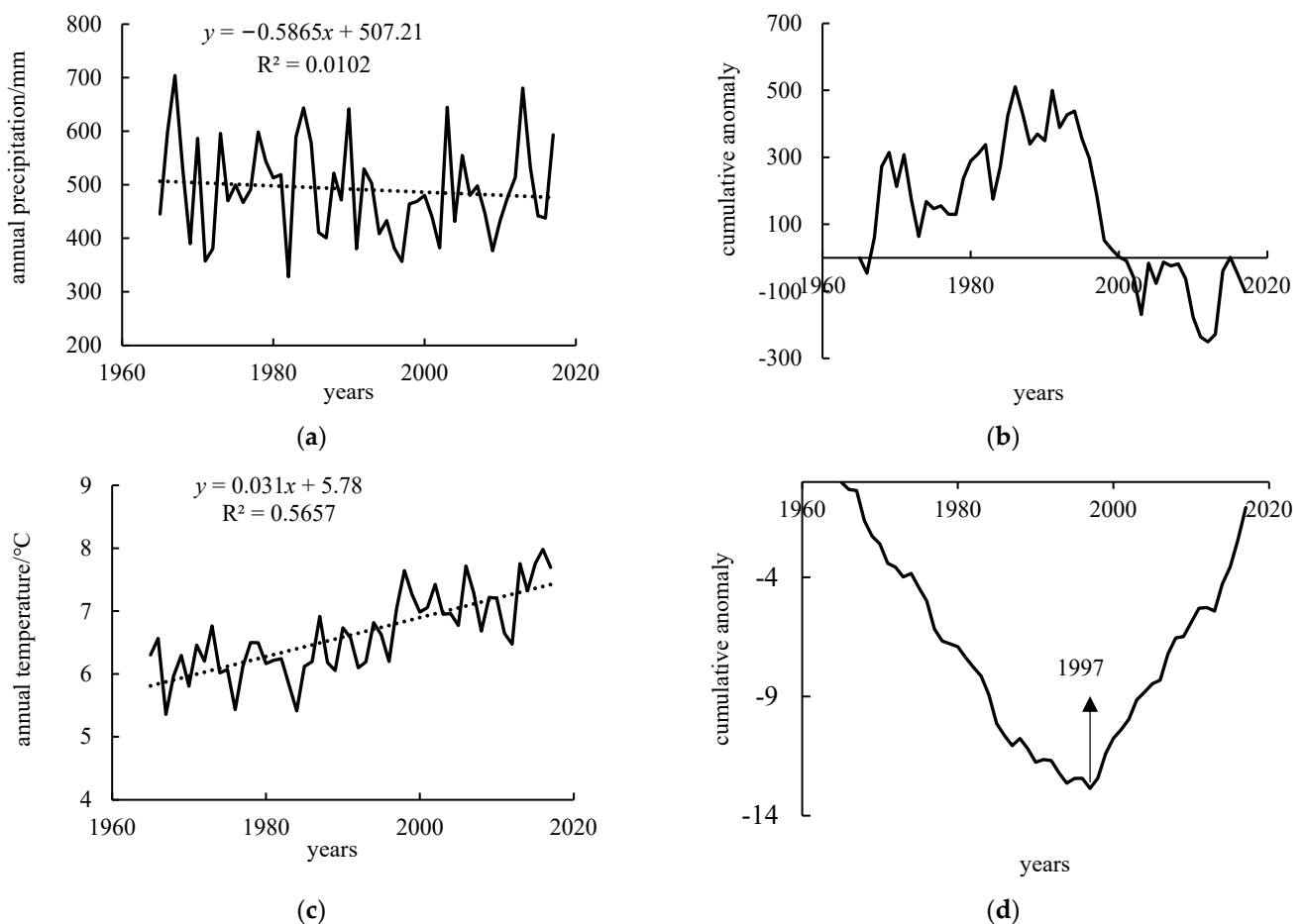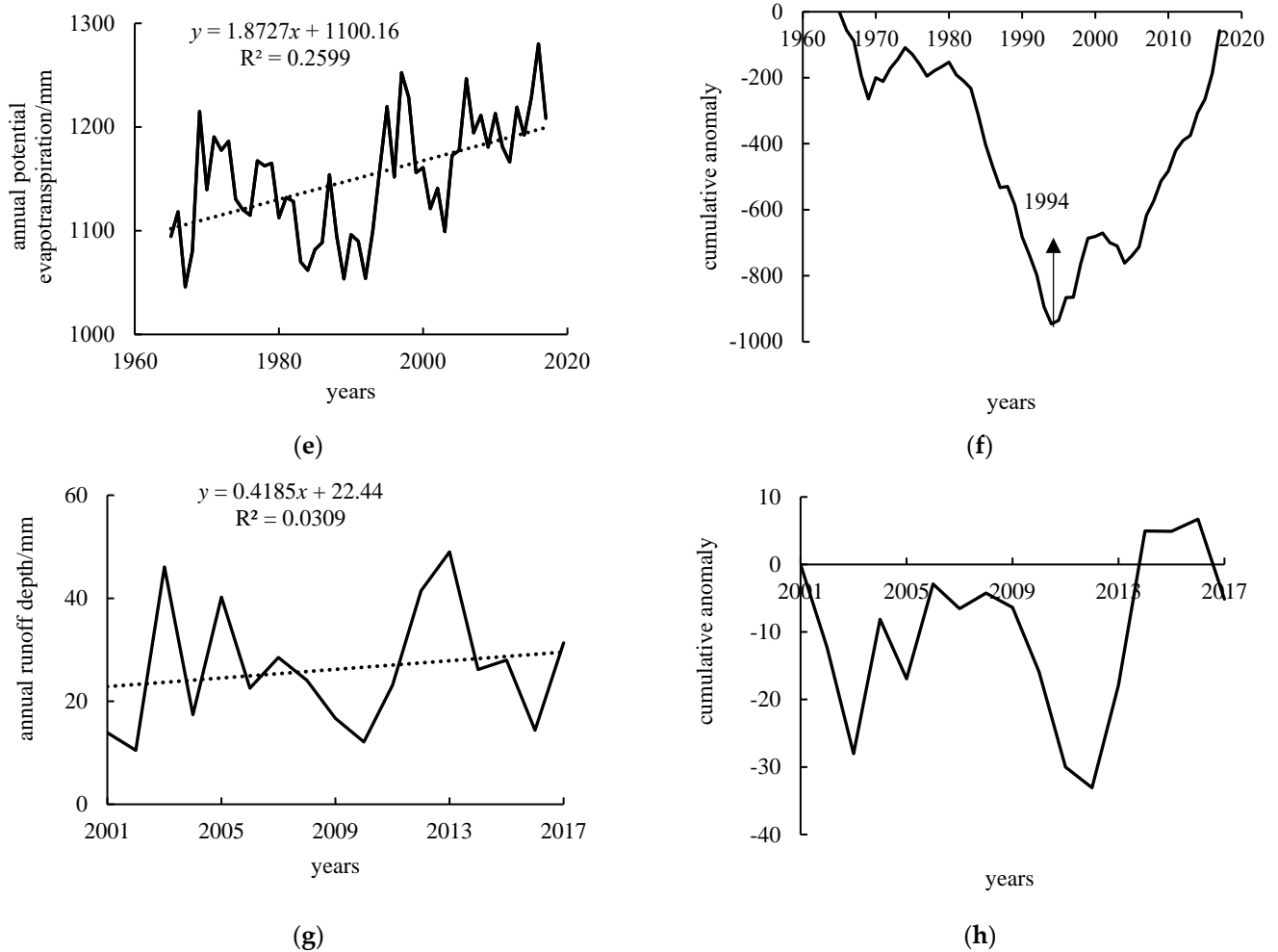

(a)

(b)

(c)

(d)

Figure 3. *Cont.*

(e)

(f)

(g)

(h)

Figure 3. Analysis of trends and abrupt changes of hydrological and meteorological elements in the basin. Note: x = year$-$1964. (**a**) Annual precipitation trend, (**b**) Analysis of abrupt change in annual precipitation, (**c**) Annual temperature trend, (**d**) Analysis of abrupt change in annual temperature, (**e**) Annual potential evapotranspiration trend, (**f**) Analysis of abrupt change in annual potential evapotranspiration, (**g**) Annual runoff depth trend, (**h**) Analysis of abrupt change in annual runoff depth.

The cumulative anomaly method was used to analyze the mutation of the annual precipitation, temperature, potential evapotranspiration and runoff depth series in the study area from 1965 to 2017. The results are shown in Figure 3. It was identified that the annual precipitation and runoff depth series did not have abrupt changes, the annual mean temperature series had a significant jump around 1997, and the annual potential evapotranspiration series had a significant jump around 1994. The simulation period is 2001–2017 and after the abrupt changes.

Figure 4 shows the changing process of the annual average NDVI series in the study area from 2001 to 2017. It shows that although the average annual NDVI value of the watershed fluctuated during the 17 years, the overall trend is significant increase, which indicates that the vegetation coverage in the study area during the 17 years was increasing continuously. Especially after 2011, the vegetation condition significantly improved. The annual NDVI value of the watershed was between 0.30 and 0.38 from 2001 to 2017. The average annual NDVI value of the watershed increased by 19.7%, and reached the maximum value of about 0.38 in 2013. Figure 5 shows the seasonality of NDVI on the monthly scale in the study area from 2001 to 2017. It shows that the vegetation change in the study area has a significant seasonality across the year. The maximum monthly NDVI in the study area

generally occurs from June to August, while the minimum monthly NDVI generally occurs from January to March.
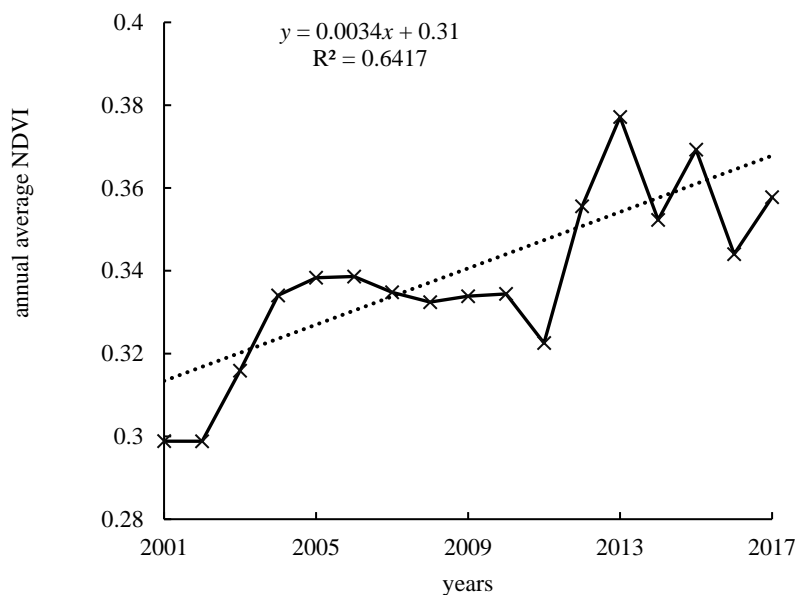

Figure 4. Annual average NDVI in the basin. Note: x = year-2000.
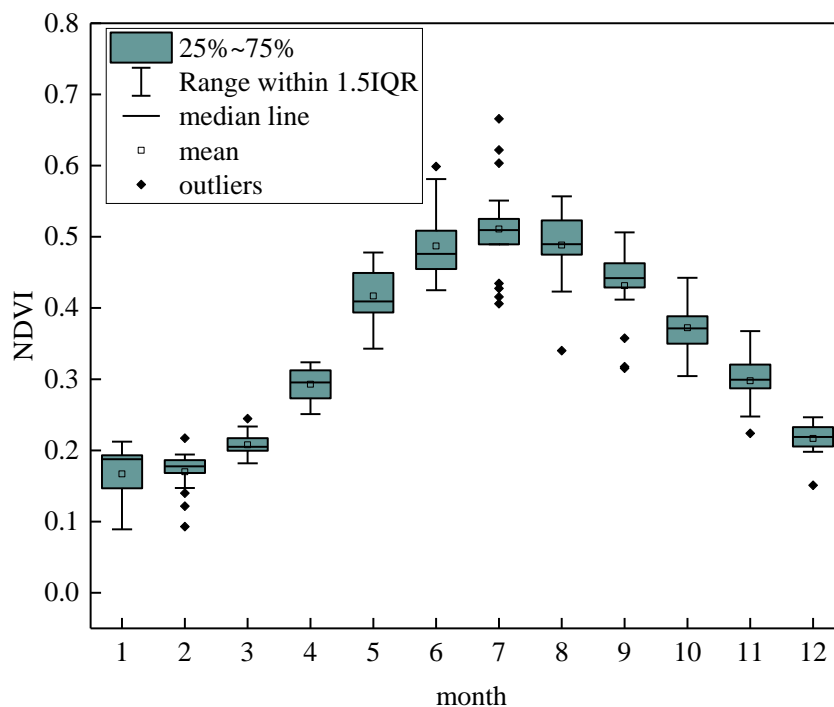

Figure 5. Seasonality of Monthly NDVI.

4.3. Simulation of the Hydrological Process

According to the mutation analysis results of the hydrometeorological data, 2001–2017 was selected as the simulation period of the model, 2001 was set as the warm-up period of the model, 2002–2013 was the calibration period, and 2014–2017 was the verification period. Sensitivity analysis was carried out on the model parameters, among which there are six parameters closely related to runoff, namely the number of runoff curves (CN2), the effective hydraulic conductivity of the main channel bed (CH_K2), the soil evaporation compensation coefficient (ESCO), and the baseflow α factor of riparian regulation and

storage (ALPHA_BNK), the Manning coefficient of the main channel (CH_N2) and the saturated hydraulic conductivity of the soil (SOL_K).

The daily runoff at the Beidao Hydrological Station is simulated, and the measured and simulated flow processes in the calibration and verification periods are shown in Figure 6, and the evaluation results of the daily flow simulation are shown in Table 1. It shows that the simulated daily flow process in the calibration period of the Beidao hydrological station is quite good, and the three evaluation indicators are all above 0.54, of which the KGE index reaches 0.70, and the simulation effect is poor in the verification period except for 2014. In general, the SWAT model has been successfully constructed in the study area, and has good applicability in the watershed. Further research is carried out based on this model.

(**a**)

(**b**)
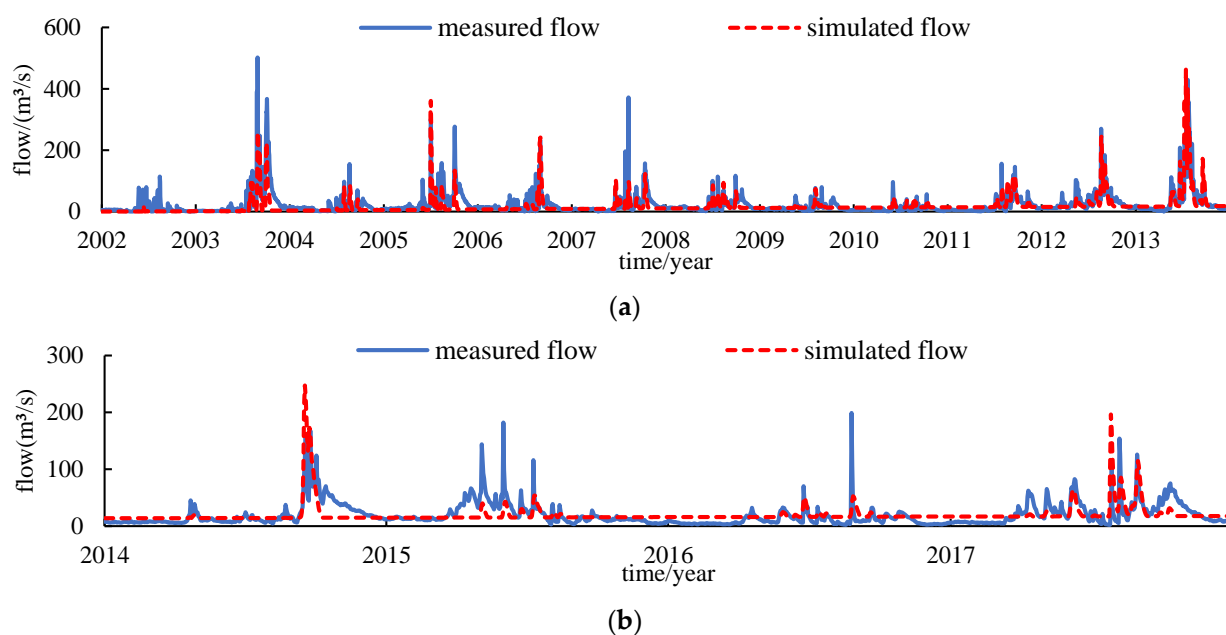
Figure 6. Results of simulated and observed streamflow in calibration period and validation period. (**a**) calibration period. (**b**) verification period.

Table 1. Evaluation result of daily flow simulation value.

| Period	R^2	NSE	KGE
Calibration period (2002–2013)	0.58	0.54	0.70
Verification period (2014–2017)	0.31	0.19	0.54

4.4. Time-Varying Parameters of the Hydrological Model

In order to obtain the time-varying parameters of the SWAT model, the SUFI-2 algorithm was used to calibrate the model parameters in each year from 2001 to 2017, and the previous year of each calibration period was used as the model warm-up period. Then, the daily runoff process of the study area in each year was simulated by the SWAT model with one parameter set of this year. The Nash–Sutcliffe efficiency coefficient, R^2 and KGE were used to evaluate the simulation accuracy of the runoff in each period. The results are shown in Table 2. It shows that the daily runoff simulation accuracy in the other 10 years met the requirements, except for the poor simulation in 2002, 2004, 2008, 2009, 2016 and 2017.

Table 2. Evaluation result of simulated daily flow of each year.

Year	R^2	NSE	KGE
2002	0.33	0.26	0.53
2003	0.74	0.73	0.77
2004	0.34	0.34	0.44
2005	0.56	0.53	0.71
2006	0.56	0.55	0.67
2007	0.42	0.42	0.52
2008	0.37	0.33	0.55
2009	0.30	0.15	0.55
2010	0.61	0.59	0.67
2011	0.53	0.52	0.58
2012	0.68	0.66	0.82
2013	0.64	0.62	0.79
2014	0.50	0.42	0.70
2015	0.45	0.44	0.62
2016	0.36	0.35	0.47
2017	0.29	0.12	0.53

The hydrological model was calibrated year by year in 1-year increments. Four time-dependent model parameter series, CN2, ESCO, ALPHA_BNK and CH_N2, were obtained for the study area. The relationship between model parameters and environmental characterization factors, i.e., precipitation, potential evapotranspiration and NDVI in the basin is plotted, as shown in Figures 7–10. It shows that the four parameters are fluctuating in different degrees during the study period. There was no obvious trend in CN2 and CH_N2. The soil evaporation compensation coefficient (ESCO) and ALPHA_BNK showed a downward trend, but the magnitude of change in ALPHA_BNK was small and negligible. The smaller the value, the more evapotranspiration water can be obtained from the lower soil layer, which is consistent with the conclusion that the watershed evaporation is increasing year by year, as shown in Figure 8.
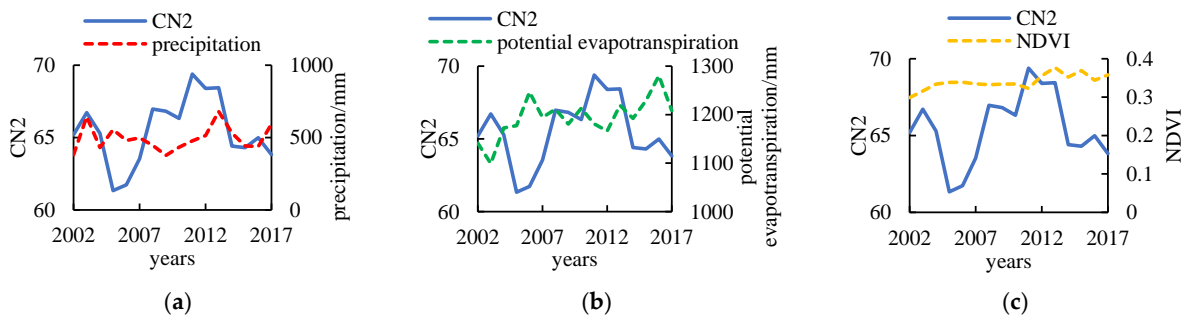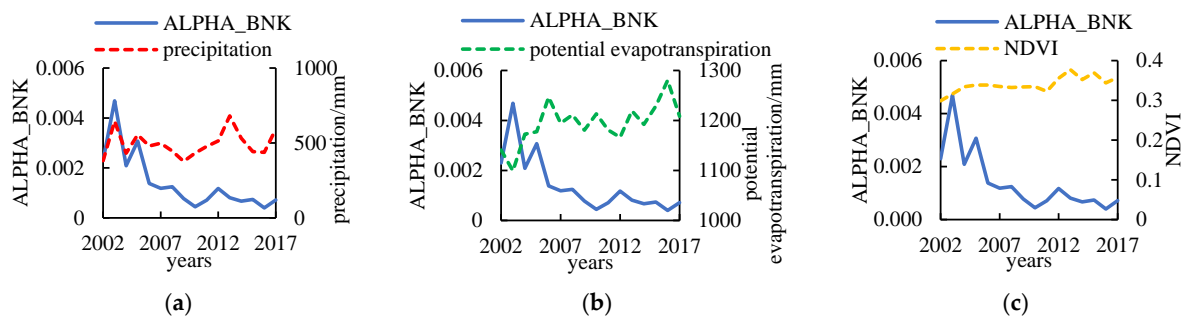

Figure 7. Time-varying process of CN2 to precipitation, potential evapotranspiration and NDVI. (**a**) Precipitation, (**b**) potential evapotranspiration, (**c**) NDVI.
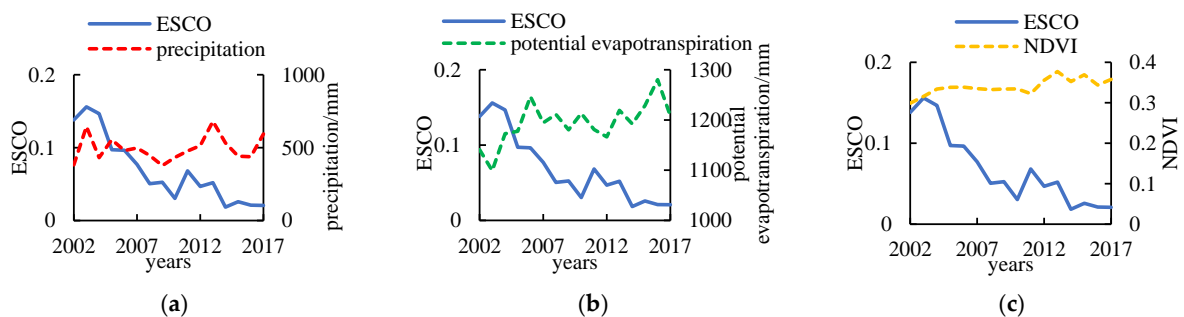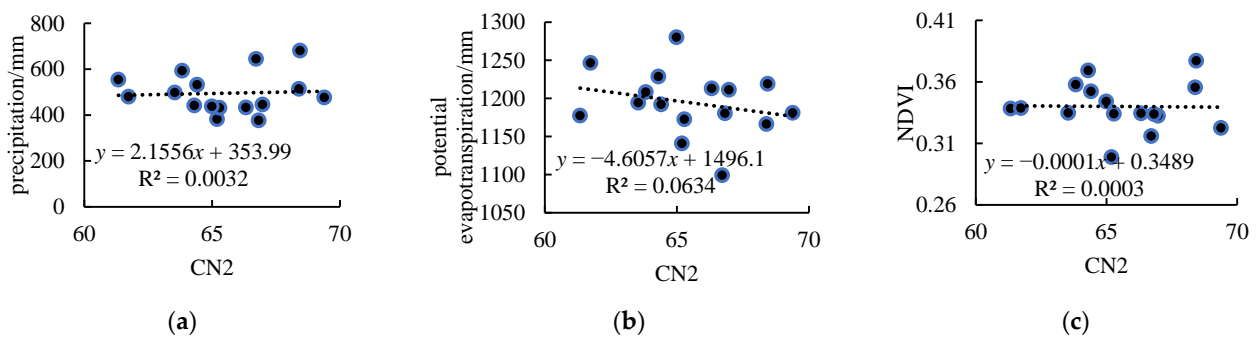

Figure 8. Time-varying process of ESCO to basin precipitation, potential evapotranspiration and NDVI. (**a**) Precipitation, (**b**) potential evapotranspiration, (**c**) NDVI.
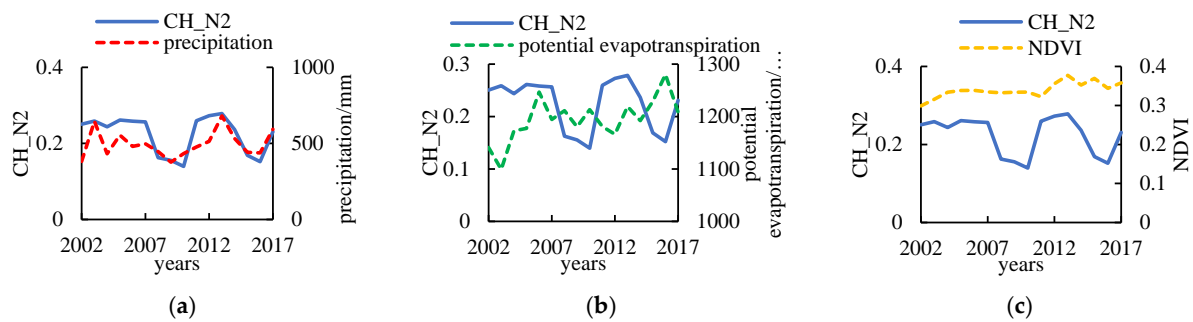
Figure 9. Time-varying process of CH_N2 to basin precipitation, potential evapotranspiration and NDVI. (**a**) Precipitation, (**b**) potential evapotranspiration, (**c**) NDVI.

Figure 10. Time-varying process of ALPHA_BNK to basin precipitation, potential evapotranspiration and NDVI. (**a**) Precipitation, (**b**) potential evapotranspiration, (**c**) NDVI.

4.5. Analysis of the Relationship between Model Parameters and Environmental Factors

The scatter plots of the hydrological model parameters and environmental representation factors of precipitation, potential evapotranspiration and NDVI were shown to identify the relationship between them, and the results are shown in Table 3, Figures 11–14. Figure 11 shows that there is a weak negative correlation between CN2 and potential evapotranspiration. The number of runoff curves (CN2) changes inversely with the change of potential evapotranspiration, and has no obvious correlation with precipitation and NDVI. In Figure 12, ESCO showed a certain negative correlation with potential evapotranspiration and NDVI, and the correlation coefficient passed the 0.05 significance level test. The soil evaporation compensation coefficient (ESCO) decreased with the increase in potential evapotranspiration and NDVI, and had no significant correlation with precipitation. The smaller the value of ESCO, the more evaporative water the model can obtain from the lower soil layer, resulting in the reduction of surface runoff, interflow and subsurface runoff, especially the most obvious reduction in surface runoff. In Figure 13, CH_N2 has a certain correlation with precipitation and potential evapotranspiration. It increases with the increase in precipitation and decreases with the increase in potential evapotranspiration. There is no obvious correlation with NDVI. The correlation coefficient between CH_N2 and precipitation passes the 0.05 significance level test. In Figure 14, ALPHA_BNK showed a certain negative correlation with potential evapotranspiration and NDVI, and the correlation coefficient passed the 0.05 significance level test. The baseflow α factor of riparian regulation and storage (ALPHA_BNK) decreased with the increase in potential evapotranspiration and NDVI, and had a weak positive correlation with precipitation. The baseflow α factor of riparian regulation and storage is a response index reflecting the discharge rate of subsurface runoff to the river discharge at the river bank, and the river discharge is positively correlated with it.

Table 3. The R^2 of each parameter with precipitation, potential evapotranspiration and NDVI.

R^2	Precipitation	Potential Evapotranspiration	NDVI
the number of runoff curves (CN2)	0.0032	0.0634	0.0003
the soil evaporation compensation coefficient (ESCO)	0.0008	0.4463 *	0.4402 *
the Manning coefficient of the main channel (CH_N2)	0.3364 *	0.2062	0.0009
the baseflow α factor of riparian regulation and storage (ALPHA_BNK)	0.1036	0.5453 *	0.2563 *

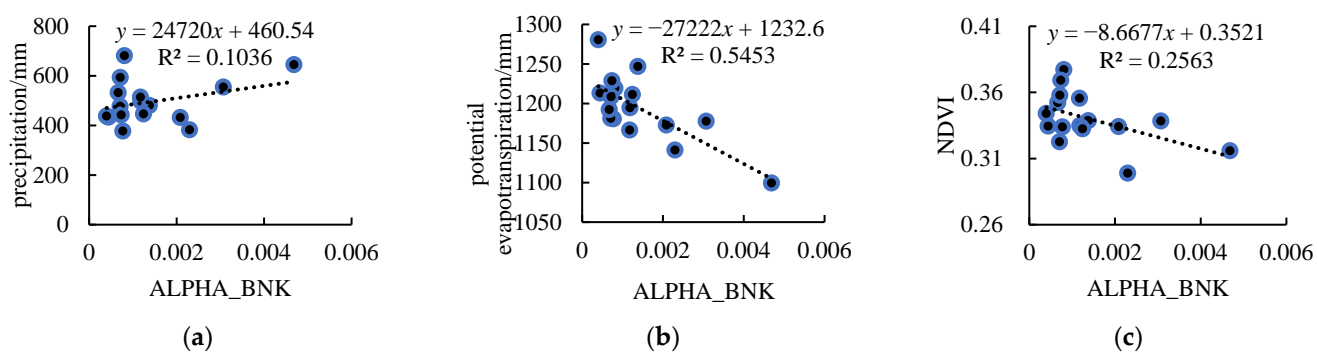Note: * Indicates passing the 0.05 significance level test.

Figure 11. Correlation of CN2 to watershed precipitation, potential evapotranspiration, NDVI. (**a**) Precipitation, (**b**) potential evapotranspiration, (**c**) NDVI.
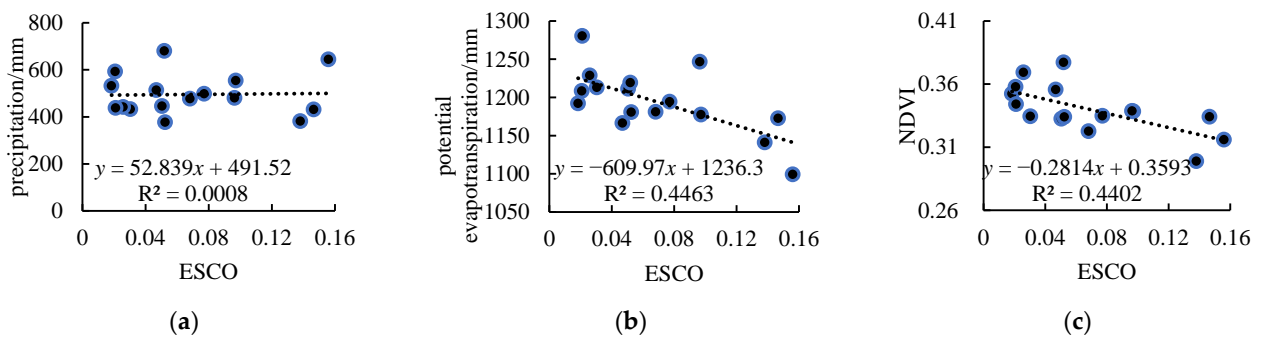
Figure 12. Correlation of ESCO to watershed precipitation, potential evapotranspiration, NDVI. (**a**) Precipitation, (**b**) potential evapotranspiration, (**c**) NDVI.
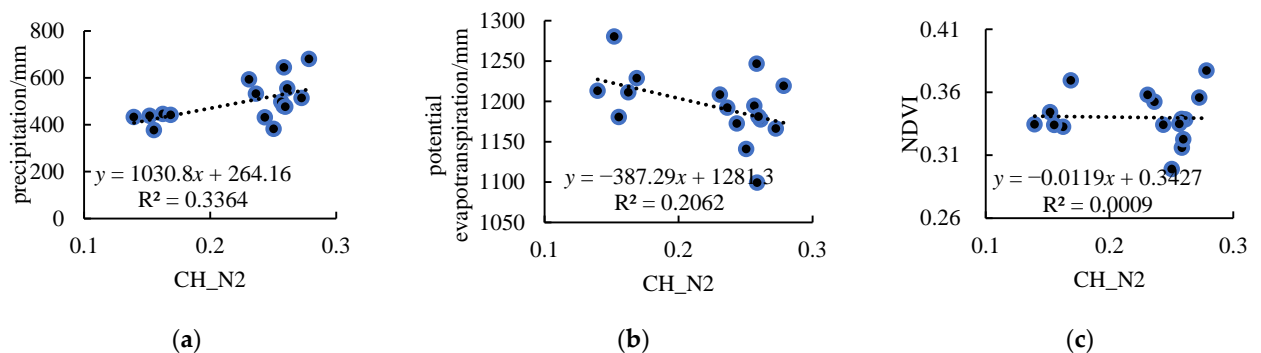
Figure 13. Correlation of CH_N2 to watershed precipitation, potential evapotranspiration, NDVI. (**a**) Precipitation, (**b**) potential evapotranspiration, (**c**) NDVI.

Figure 14. Correlation of ALPHA_BNK to watershed precipitation, potential evapotranspiration, NDVI. (**a**) Precipitation, (**b**) potential evapotranspiration, (**c**) NDVI.

In summary, all four parameters of the SWAT model in the upper reach of the Wei River Basin show a certain correlation with potential evapotranspiration, and some parameters have a correlation with precipitation or NDVI, which indicates that the changes of the hydrological model parameters in the upper reach of the Wei River Basin are closely related to the dynamic changes of potential evapotranspiration. Therefore, potential evapotranspiration can be used as a representative factor of the dynamic change of model parameters.

5. Conclusions

In this study, the upper reach of the Wei River is selected as the study area, and the temporal and spatial evolution of the ecological hydrometeorological elements in the study area is revealed using the linear regression method and the cumulative anomaly method. The time-varying parameter series of the hydrological model is obtained based on the SWAT model in each year. The time-varying characteristics of the model parameters and environmental indicators such as precipitation, potential evapotranspiration and NDVI were analyzed, and the response relationship between them was identified.

In addition to the decreasing trend of annual precipitation in the basin, the hydrometeorological elements such as annual potential evapotranspiration, annual average temperature, annual runoff depth and annual average NDVI all showed an increasing trend. The annual precipitation and annual runoff depth series in the basin did not change abruptly, but the annual mean temperature series and the annual potential evapotranspiration series jumped significantly around 1997 and 1994, respectively.

Except for the six years of 2002, 2004, 2008, 2009, 2016 and 2017 in 2002–2017, the daily runoff simulation accuracy in the other 10 years met the requirements. The four model parameters of CN2, ESCO, CH_N2 and ALPHA_BNK all fluctuated with time during the study period. The number of runoff curves (CN2) and CH_N2 had no obvious trend changes, while ESCO and ALPHA_BNK showed a downward trend. Because the magnitude of change in ALPHA_BNK was small, it can be neglected, and the change of ESCO is consistent with the conclusion that the evaporation in the basin increases year by year.

All model parameters show a certain correlation with potential evapotranspiration in the basin, which indicates that the changes of the hydrological model parameters in the upper reach of the Wei River Basin are closely related to the dynamic changes of potential evapotranspiration. Therefore, potential evapotranspiration can be used as an environmental factor to characterize the dynamic changes of the model parameters.

References

1. Tang, Q.H. Global change hydrology: Terrestrial water cycle and global chang. *Sci. China Earth Sci.* **2020**, *63*, 459–462. [CrossRef]
2. Campbell, J.L.; Driscoll, C.T.; Pourmokhtarian, A.; Hayhoe, K. Streamflow responses to past and projected future changes in climate at the Hubbard Brook Experimental Forest, New Hampshire, United States. *Water Resour. Res.* **2011**, *47*, 1198–1204. [CrossRef]
3. Zhang, L.; Liu, D.; Zhang, H.; Huang, Q.; Meng, X. Impact of climate change and human activities on runoff variation in Beiluo River basin. *J. Hydroelectr. Eng.* **2016**, *35*, 55–66.
4. IPCC. Climate Change 2013: The Physical Science Basis. In *Contribution of Working Group I to the Fifth Assessment Report of the Intergovernmental Panel on Climate Change*; Cambridge University Press: Cambridge, NY, USA, 2013.
5. Dore, M.H.I. Climate change and changes in global precipitation patterns: What do we know? *Environ. Int.* **2005**, *31*, 1167–1181. [CrossRef] [PubMed]
6. Jingyi, D.I.N.G.; Wenwu, Z.H.A.O.; Jun, W.A.N.G. Scale effect of the impact on runoff of variations in precipitation/vegetation: Taking northern Shaanxi loess hilly-gully region as an example. *Prog. Geogr.* **2015**, *34*, 1039–1051.
7. Brown, A.E.; Western, A.W.; McMahon, T.A.; Zhang, L. Impact of forest cover changes on annual streamflow and flow duration curves. *J. Hydrol.* **2013**, *483*, 39–50. [CrossRef]
8. Coe, M.T.; Latrubesse, E.M.; Ferreira, M.E.; Amsler, M.L. The effects of deforestation and climate variability on the streamflow of the Araguaia River, Brazil. *Biogeochemistry* **2011**, *105*, 119–131. [CrossRef]
9. Collier, C.G. The impact of urban areas on weather. *Q. J. R. Meteorol. Soc.* **2006**, *132*, 1–25. [CrossRef]
10. Cheng, C.K.M.; Chan, J.C.L. Impacts of land use changes and synoptic forcing on the seasonal climate over the Pearl River Delta of China. *Atmos. Environ.* **2012**, *60*, 25–36. [CrossRef]
11. Weiskel, P.K.; Vogel, R.M.; Steeves, P.A.; Zarriello, P.J.; DeSimone, L.A.; Ries, K., III. Water use regimes: Characterizing direct human interaction with hydrologic systems. *Water Resour. Res.* **2007**, *43*, W04402. [CrossRef]
12. Patterson, L.A.; Lutz, B.; Doyle, M.W. Climate and direct human contributions to changes in mean annual streamflow in the South Atlantic, USA. *Water Resour. Res.* **2013**, *49*, 7278–7291. [CrossRef]
13. Milly, P.C.; Betancourt, J.; Falkenmark, M.; Hirsch, R.M.; Kundzewicz, Z.W.; Lettenmaier, D.P.; Stouffer, R.J. Stationarity is dead: Whither water management? *Science* **2008**, *319*, 573–574. [CrossRef]
14. Lihua, X.I.O.N.G.; Shuonan, L.I.U.; Bin, X.I.O.N.G.; Wentao, X.U. Impacts of vegetation and human activities on temporal variation of the parameters in a monthly water balance model. *Adv. Water Sci.* **2018**, *29*, 625–635.
15. Liu, S.N. *Temporal Variation of the Parameters in a Monthly Water Balance Model*; Wuhan University: Wuhan, China, 2019.
16. Wang, J.; Wang, Z.; Cheng, H.; Kang, J.; Liu, X. Land Cover Changing Pattern in Pre-and Post-Earthquake Affected Area from Remote Sensing Data: A Case of Lushan County, Sichuan Province. *Land* **2022**, *11*, 1205. [CrossRef]
17. Kang, J.; Wang, Z.; Cheng, H.; Wang, J.; Liu, X. Remote Sensing Land Use Evolution in Earthquake-Stricken Regions of Wenchuan County, China. *Sustainability* **2022**, *14*, 9721. [CrossRef]
18. Deng, C. *Study of Temporal Variability of Model Parameters in Monthly Water Balance Modeling*; Wuhan University: Wuhan, China, 2017.
19. Kingumbi, A.; Bargaoui, Z.; Ledoux, E.; Besbes, M.; Hubert, P. Hydrological stochastic modelling of a basin affected by land-use changes: Case of the Merguellil basin in central Tunisia. *Hydrol. Sci. J.* **2007**, *52*, 1232–1252. [CrossRef]
20. Vaze, J.; Post, D.A.; Chiew FH, S.; Perraud, J.M.; Viney, N.R.; Teng, J. Climate non-stationarity-validity of calibrated rainfall–runoff models for use in climate change studies. *J. Hydrol.* **2010**, *394*, 447–457. [CrossRef]

21. Merz, R.; Parajka, J.; Blöschl, G. Time stability of catchment model parameters: Implications for climate impact analyses. *Water Resour. Res.* **2011**, *47*, 2144–2150. [CrossRef]
22. Sun, Y. *Time Instability of Hydrological Model Parameters under Changing Environment*; Tsinghua University: Beijing, China, 2015.
23. Brigode, P.; Oudin, L.; Perrin, C. Hydrological model parameter instability: A source of additional uncertainty in estimating the hydrological impacts of climate change? *J. Hydrol.* **2013**, *476*, 410–425. [CrossRef]
24. Wallner, M.; Haberlandt, U. Non-stationary hydrological model parameters: A framework based on SOM-B. *Hydrol. Process.* **2015**, *29*, 3145–3161. [CrossRef]
25. Wu, H.Z.; Liu, D.F.; Huang, Q.; Zheng, H.W.; Zou, H.; Ye, N.; Lin, M. Study on accuracy evaluation and substitutability of multiple precipitation products on Loess Plateau. *J. Hydroelectr. Eng.* **2021**, *40*, 31–40.
26. Jiang, Y.; Xu, Z.X.; Wang, J. Comparison among five methods of trend detection for annual runoff series. *Shuili Xuebao* **2020**, *51*, 845–857.
27. Zhang, Y.H.; Song, X.F. Techniques of abrupt change detection and trends analysis in hydroclimatic time-series: Advances and evaluation. *Arid. Land Geogr.* **2015**, *38*, 652–665.
28. Hotchkiss, R.H.; Jorgensen, S.F.; Stone, M.C.; Fontaine, T.A. Regulated river modeling for climate change impact assessment: The Missouri river. *J. Am. Water Resour. Assoc.* **2000**, *36*, 375–386. [CrossRef]
29. Yang, J.; Reichert, P.; Abbaspour, K.C.; Xia, J.; Yang, H. Comparing uncertainty analysis techniques for a SWAT application to the Chaohe Basin in China. *J. Hydrol.* **2008**, *358*, 1–23. [CrossRef]
30. Chaefli, B.; Gupta, H.V. Do Nash values have value. *Hydrol. Process. Int. J.* **2007**, *21*, 2075–2080. [CrossRef]
31. Moriasi, D.N.; Arnold, J.G.; Van Liew, M.W.; Bingner, R.L.; Harmel, R.D.; Veith, T.L. Model evaluation guidelines for systematic quantification of accuracy in watershed simulations. *Trans. ASABE* **2007**, *50*, 885–900. [CrossRef]
32. Gupta, H.V.; Kling, H.; Yilmaz, K.K.; Martinez, G.F. Decomposition of the mean squared error and NSE performance criteria: Implications for improving hydrological modelling. *J. Hydrol.* **2009**, *377*, 80–91. [CrossRef]
33. Kling, H.; Fuchs, M.; Paulin, M. Runoff conditions in the upper Danube basin under an ensemble of climate change scenarios. *J. Hydrol.* **2012**, *424*, 264–277. [CrossRef]